August, 2008

The Dependence of Measured Modulation Error Ratio on Phase Noise

Ron D Katznelson, *Bi-Level Technologies*

The Dependence of Measured Modulation Error Ratio on Phase Noise

Ron D. Katznelson *

Abstract **— This paper reviews the algorithms used by Vector Signal Analyzers to measure Modulation Error Ratio (MER) and derives the explicit functional dependence of measured MER on phase noise of digital transmitters. The modulation error model is introduced and the analytical expression for key estimated parameters required to obtain MER measure are derived. The essential elements of algorithms employed by MER measurement instruments to estimate amplitude scale, frequency offset, and initial phase intercept and the resulting MER are identified. The frequency response of the effective phase-noise rejection filtering action associated with a given measurement epoch is derived. It is shown that this effective rejection filter has a second-order high-pass characteristics in MER instruments that use linear phase trajectory estimation. This result is subsequently applied in analyzing a typical Lorentzian density phase noise profile to obtain an explicit expression for phase-noise-induced MER values as a function of measurement block duration. Finally, certain implications of this study to MER measurement and specification practices including the Data-Over-Cable Service Interface Specifications (DOCSIS®) are identified.**

Index of terms **— MER, Modulation Error Ratio, EVM, Error Vector Magnitude, QAM, Phase Noise, Lorentzian density, DOCSIS, Vector Signal Analyzer.**

I. INTRODUCTION

The ultimate figure of merit for impairments in digital communication links is the deviation of actual received constellation vectors from an ideal reference constellation. Thus, the relevant metric of digital modulation accuracy is the Error Vector Magnitude (EVM), which represents the distance between measured and ideal modulation vectors [1]. This measure encompasses the effects caused by magnitude and phase distortions. The Modulation Error Ratio (MER) is an inversely related metric to EVM squared, conveying the same information but having the intuitive representation of signal-to-noise ratio. MER is the ratio of the average symbol power to average error power and is often expressed in dB. Because MER represents the power addition of all distortion errors including spurious noise, the industry embraced the MER measure as the operative criteria encompassing all the in-channel errors in one relevant measure from which bit error rate can be predicted. This paper focuses on an aspect of MER that received very little attention in the literature - the MER measures

*Manuscript received August_, 2008. An earlier version of this paper was distributed in 2005 as a contribution to CableLabs'® Working Group on Data Over Cable Service Interface Specifications (DOCSIS®). At that time, the Author was with Broadband Innovations, San Diego, CA. He is now with Bi-Level Technologies, Encinitas, CA (email: ron@bileveltech.com).

resulting solely from phase errors due to phase noise of oscillators used in the communication link. The ability to predict these phase noise effects can help establish upper bounds for MER measures that are otherwise free from all other impairments.

Two general categories of commercially available MER measuring instruments are distinguished by the method for establishing their internal reference symbol constellation. The first type employs a precision receiver-demodulator with continuously running carrier recovery and symbol timing loops as normally found in commercial modems. Some instruments in this first category may provide user selection among a couple of hardwired carrier tracking loop bandwidth settings. The second and more versatile category of MER measuring instruments are vector signal analyzers that acquire a block of digital raw samples during a measurement run. The block of samples is fed to digital signal processing software routines, which derive the appropriate parameters including carrier frequency offset, phase, amplitude, and symbol timing. Based on these estimated parameters that establish the presumed ideal constellation points, the MER software routine calculates an MER measure expressing the deviations from such presumed ideal vector points. A significant advantage of instruments in this second category is that they provide flexibility in setting detection parameters including samples per symbol and symbol block length. Because these vector signal analyzers operate on blocks of data samples and do not require continuous demodulation, they permit measurements of signals under bursty data protocols.

The possible settings of MER instruments' measurement modes affecting carrier phase tracking such as symbol block length, produce a range of susceptibilities to phase noise. However, there appears to be a paucity of published analytical treatment of the phase noise effects on measured MER. Previous work only assumes a *given total* phase noise error from the presumed ideal reference constellation, from which analytical results are derived showing that the relative error power is proportional to total phase noise power [2],[3]. However, these prior studies appear to assume that MER measurement instruments can somehow divine the ideal reference constellation from which MER measures are obtained. They ignore the fact that such measurements involve the estimation of the parameters of the constellations based on noisy data, thereby introducing phase-noise-dependent 'definition' of what constitutes an "error". Thus, previous studies do not derive the MER values based on the phase noise spectral density and the symbol block length used by the instrument, wherein *only a portion* of the total phase noise energy is actually reflected in the MER.

Vendors of MER measuring instruments also appear silent on the numerical impact on MER measures by a specific choice of carrier phase tracking conditions such as the symbol block length. One such vendor apparently only identifies factors *other than* phase noise as considerations for selecting the symbol block size. It recommends setting the “Result Length” for bursted signals so as not to include data symbols taken before or after the burst [1]. It is therefore the purpose of this paper to rigorously derive the explicit numerical effects of phase noise on measured MER and its dependence on symbol block duration. We derive the results in the context of Quadrature Amplitude Modulation (QAM) signals although it can be shown that the results are essentially independent of the exact form of the modulation constellation.

This paper is organized as follows: Section II introduces the definition of MER and the phase noise model including the parameters that must be estimated by MER measurement instruments to obtain the MER measure. Section III derives the essential elements of the algorithms employed by MER measurement instruments to estimate the relevant constellation parameters and the resulting MER. The frequency response of the effective phase-noise rejection filtering associated with a given measurement block size is analytically derived. This result is subsequently applied for a typical Lorentzian density phase noise profile to obtain an explicit expression for phase-noise induced MER degradation as a function of measurement block duration. Finally, Section IV identifies certain implications of this study to MER measurement and specification practices including its contribution to the Data-Over-Cable Service Interface Specifications (DOCSIS®).

II. MER AND THE PHASE NOISE MODEL

In the receiving device, a QAM signal is assumed to be received by an ideal quadrature demodulator employing a filter matched to the transmitter impulse response for each quadrature component, followed by a sampler at the correct symbol sampling times. We further assume that the digital demodulator incorporates a symbol-time recovery system that derives the optimal sampling rate and times, thereby assuming no timing error contributions to MER. These samples are each provided in two phase-quadrature components and represented by complex numbers. In ideal conditions, for every sample (sequentially indexed by k), these complex numbers or vectors (denoted by Z_k) fall on discrete points of the reference QAM constellation having discrete symbol points with nearest-neighbor voltage separation of $2d$:

$$Z_k = p_k d + i q_k d \quad p_k = \pm 1, \pm 3, \pm 5, \pm 7, \ldots; \; q_k = \pm 1, \pm 3, \pm 5, \pm 7, \ldots; \text{ and where } i = \sqrt{-1} \tag{1}$$

We assume that the random integers p_k and q_k are jointly uncorrelated and that each outcome in their respective range is equally likely. Over an observation period containing N contiguous statistically uncorrelated symbols, the transmitted vector signal may be subject to phase fluctuations φ_k and additive complex noise and distortion components w_k and is thus represented by an observed vector samples V_k given by

$$V_k = e^{i\varphi_k} Z_k + w_k \tag{2}$$

A measurement run involves generating and transmitting a random sequence of symbols comprised of a long pseudorandom sequence of integers p_k and q_k. After the MER instrument has acquired the signal and has stabilized, an ensemble of records, each N symbols long, is captured and processed. In order to measure the MER, the device must first derive the 'best match' between its internal reference constellation points Z_k and the received signal vector V_k by estimating the constellation parameters discussed below. For each such record captured, the MER measurement device obtains the received symbols' distance from the presumed noise-free reference constellation based on (2) and it estimates a mean-squared-error measure given by H as follows:

$$H = \sum_{k=1}^{N} \left| V_k - \hat{a}\, e^{i\hat{\varphi}_k} Z_k \right|^2 = \sum_{k=1}^{N} [\left|V_k\right|^2 + \hat{a}^2 \left|Z_k\right|^2 - 2\hat{a}\,\mathrm{Re}\,(e^{i\hat{\varphi}_k} Z_k V_k^*)] \tag{3}$$

where the parameter $\hat{a}$ is a single amplitude scale estimate for the full record of N consecutive symbols and where $\hat{\varphi}_k$ is phase trajectory estimate accounting for possible phase drifts over the observation of the N consecutive symbols. Because the MER instrument only observes the received samples V_k, it does not have *a priori* knowledge of the randomly transmitted symbols Z_k and it uses the decision-directed values based on its received symbols' decision regions. Some instruments may instead use the knowledge of the pseudorandom sequence employed by the test modulated signal generator after having frame-synchronized to it. In this analysis, we assume that such symbol detection error rate is negligible so that the MER instrument obtains the correct symbols Z_k from which it constructs the squared error H in (3). A set of parameters $\hat{a}$ and $\hat{\varphi}_k$, are estimated by the MER measuring device for every captured record of N consecutive symbols. The parameters that minimize the magnitude squared of H are selected for each record and as such, they are random variables depending on the random phases φ_k and implicitly on the transmitted random sequence of symbols Z_k. The resulting minimal relative level of H as derived is used to compute the MER value for that record. Averaging over an ensemble of MER values for each record establishes the resultant displayed MER value, as defined below:

$$MER^{-1} \equiv E\left[\frac{\min_{\hat{a},\,\hat{\varphi}_k} H}{\sum_{k=1}^{N} |Z_k|^2}\right] \cong \frac{E\left[\min_{\hat{a},\,\hat{\varphi}_k} H\right]}{E\left[\sum_{k=1}^{N} |Z_k|^2\right]} \tag{4}$$

where E denotes the statistical expectation. The approximation on the right hand side of (4) is most valid for long enough symbol record lengths (large values of N), for which the standard deviation of the sample record energy $\sum_{k=1}^{N} |Z_k|^2$ is sufficiently small compared to its expectation so that the expectation of the ratio can be replaced by the ratio of the expectations. Most researchers and instrument designers define the average MER directly by the right hand side of (4) and we shall adopt this approximation for our results below.

III. ESTIMATION OF MER AND RELATED PARAMETERS

All MER measuring instruments essentially have in common the general process described above but they may differ in the manner in which they perform signal acquisition (i.e. symbol time and carrier recovery) and the method by which they derive the phase trajectory estimates $\hat{\varphi}_k$. In what follows, we will analyze systems that computationally derive phase parameter estimates based on finite length epochs of symbols and that use a first order linear phase trajectory model, as expected from any ideal modulation source having no phase noise but only an unknown frequency offset Ω. One such commercial measurement system has gained considerable adoption by the industry and the details of its early version are described in a patent to Birgenheier et al. [4]. Only two parameters need be estimated in order to describe the estimated phase trajectory $\hat{\varphi}_k$ for every symbol k:

$$\hat{\varphi}_k = \hat{\varphi}_0 + k\hat{\Omega}T_S \tag{5}$$

The two parameters are the phase intercept estimate $\hat{\varphi}_0$ and the angular frequency-offset estimate $\hat{\Omega}$. T_S is the symbol duration, assumed to be known by the instrument with negligible error, as symbol rate is properly acquired. Any deviations of the actual measured random phase φ_k from the phase trajectory estimate $\hat{\varphi}_k$ would represent constellation noise degradation from a presumed ideal source and would therefore contribute to the measured MER. For purposes of assessing the phase noise effects on MER at relatively high signal-to-noise ratios after carrier and symbol time tracking system convergence, we note that many practical estimation methods have asymptotically identical performance results (and therefore the same phase noise effects on measured MER) as they all asymptotically constitute Maximum Likelihood Estimators under Gaussian noise. Therefore, at sufficiently high signal-to-noise ratios, the various computational procedures commercially employed to obtain these estimates and the resultant MER values are essentially equivalent to the method of least square regression of the received data. Hence, we apply this minimum squared error estimation criterion to derive and evaluate these computational procedures' performance under phase noise conditions. To derive these estimators, we seek the mathematical conditions for attaining the minimum in (4) above. Based on the expression for H in (3), the necessary conditions for a minimum are formally given by

$$\frac{\partial H}{\partial \hat{a}} = 2\sum_{k=1}^{N}[\hat{a}\left|Z_k\right|^2 - \mathrm{Re}\,(e^{i\hat{\varphi}_k} Z_k V_k^*)] = 0 \tag{6}$$

$$\frac{\partial H}{\partial \hat{\varphi}_0} = -2\hat{a}\sum_{k=1}^{N}\mathrm{Re}\,(i\, e^{i\hat{\varphi}_k} Z_k V_k^*) = 0 \tag{7}$$

$$\frac{\partial H}{\partial \hat{\Omega}} = -2\hat{a}\,T_S\sum_{k=1}^{N}\mathrm{Re}\,(i\,k\, e^{i\hat{\varphi}_k} Z_k V_k^*) = 0 \tag{8}$$

Equations (7) and (8) were obtained by substituting (5) in (3). Now, (6) readily provides the amplitude scale estimate $\hat{a}$ in terms of the observed vectors V_k:

$$\hat{a} = \sum_{k=1}^{N}\mathrm{Re}\,(e^{i\hat{\varphi}_k} Z_k V_k^*) \Big/ \sum_{k=1}^{N}\left|Z_k\right|^2 \tag{9}$$

It is now possible to eliminate $\hat{a}$ in (3) by substituting the result of (9):

$$H = \sum_{k=1}^{N}[\left|V_k\right|^2 + \hat{a}^2\left|Z_k\right|^2 - 2\hat{a}\,\mathrm{Re}\,(e^{i\hat{\varphi}_k} Z_k V_k^*)] = \sum_{k=1}^{N}\left|V_k\right|^2 - \left[\sum_{k=1}^{N}\mathrm{Re}\,(e^{i\hat{\varphi}_k} Z_k V_k^*)\right]^2 \Big/ \sum_{k=1}^{N}\left|Z_k\right|^2 \tag{10}$$

We note that system designs of MER measuring devices typically adopt programmatic procedures on the received samples V_k (and their related phase values φ_k) for deriving the estimates $\hat{a}$, $\hat{\varphi}_0$ and $\hat{\Omega}$ based on the mathematical assumption of zero additive noise. These approaches are effective because they produce unbiased estimates, at least asymptotically. In these assumed structures, solving jointly for the two remaining phase and frequency offset estimates produces solutions for $\hat{\varphi}_k$ that are independent of $\hat{a}$, and that are subsequently used in (10). These solutions can be obtained by using the phase observables φ_k of the received samples V_k in the noiseless version ($w_k = 0$) of (2) by inserting them in (7) and (8):

$$-\sum_{k=1}^{N} \mathrm{Re}\,(i\,e^{i\hat{\varphi}_k} Z_k V_k^*) = -\sum_{k=1}^{N} \mathrm{Re}\,(i\,e^{i\hat{\varphi}_k} Z_k Z_k^* e^{-i\varphi_k}) = \sum_{k=1}^{N} |Z_k|^2 \sin(\hat{\varphi}_k - \varphi_k) = 0 \tag{11}$$

$$-\sum_{k=1}^{N} \mathrm{Re}\,(i\,k\,e^{i\hat{\varphi}_k} Z_k V_k^*) = -\sum_{k=1}^{N} k\,\mathrm{Re}\,(i\,e^{i\hat{\varphi}_k} Z_k Z_k^* e^{-i\varphi_k}) = \sum_{k=1}^{N} |Z_k|^2 k \sin(\hat{\varphi}_k - \varphi_k) = 0 \tag{12}$$

As the MER measuring system converges after initial acquisition of the signal, the estimates improve in accuracy and the actual phase deviations from the estimates are sufficiently small so that $\sin(\hat{\varphi}_k - \varphi_k)$ in (11) and (12) can be approximated by $\hat{\varphi}_k - \varphi_k$. Using this approximation and substituting $\hat{\varphi}_k$ of (5) in (11) and (12), we obtain the following set of two linear equations for the two unknowns $\hat{\varphi}_0$ and $\hat{\Omega}$:

$$\hat{\varphi}_0 \sum_{k=1}^{N} |Z_k|^2 + \hat{\Omega} T_S \sum_{k=1}^{N} k |Z_k|^2 - \sum_{k=1}^{N} \varphi_k |Z_k|^2 = 0 \tag{13}$$

$$\hat{\varphi}_0 \sum_{k=1}^{N} k |Z_k|^2 + \hat{\Omega} T_S \sum_{k=1}^{N} k^2 |Z_k|^2 - \sum_{k=1}^{N} k\,\varphi_k |Z_k|^2 = 0 \tag{14}$$

For brevity, we define the symbol record moments μ_j by

$$\mu_j \equiv \sum_{k=1}^{N} k^j \,|\, Z_k \,|^2 \tag{15}$$

Using this definition, we recognize that μ_0, μ_1 and μ_2 are the linear coefficients of the unknowns in (13) and (14), the solution of which in vector form is given by:

$$\begin{bmatrix} \hat{\varphi}_0 \\ \hat{\Omega} T_S \end{bmatrix} = \frac{1}{\mu_0 \mu_2 - \mu_1^2} \begin{bmatrix} \mu_2 & -\mu_1 \\ -\mu_1 & \mu_0 \end{bmatrix} \begin{bmatrix} \sum_{k=1}^{N} \varphi_k \,|\, Z_k \,|^2 \\ \sum_{k=1}^{N} k\,\varphi_k \,|\, Z_k \,|^2 \end{bmatrix} \tag{16}$$

In this way, the unknown parameters are estimated based on the observables φ_k and the corresponding detected symbols Z_k. It should be noted that the values of φ_k in (16) must be their fully unwrapped rotational angles starting at the beginning of the measurement epoch and not their modulo-2π values. It is expected that upon convergence and correction of the instrument's frequency offset and initial phase intercept, no wrap-around of phase would be encountered over practical measurement block durations.

A. A Typical MER Estimation Algorithm

The operation of a typical MER measuring device's program implements a decision directed process for each block of N consecutive symbols with an outline essentially equivalent to the following:

(a) Receiving vectors V_k and demodulating each symbol k in the block of N symbols. This is done based on decision regions of the operating reference constellation, to determine the presumed transmitted symbol value Z_k.

(b) Using the sequence of detected symbols Z_k to form the record moments μ_j for j = 0,1,2 in accordance with (15).

(c) Deriving the phase observables φ_k from the received samples V_k based on (2), assuming maximum likelihood estimation (i.e., $w_k = 0$):

$$\varphi_k = \arctan\left(\frac{\mathrm{Im}(V_k / Z_k)}{\mathrm{Re}(V_k / Z_k)}\right) \tag{17}$$

(d) Substituting in (16) the values derived in steps (a) through (c) above to obtain the phase intercept estimate $\hat{\varphi}_0$ and the frequency-offset estimate $\hat{\Omega}$.

(e) Deriving the array of phase estimates $\hat{\varphi}_k$ based on (5) and the values of $\hat{\varphi}_0$ and $\hat{\Omega}$, and substituting $\hat{\varphi}_k$ in (9) in order to obtain the amplitude scale estimate $\hat{a}$.

(f) Using the estimates $\hat{\varphi}_k$ derived in step (e) above by inserting them in (10), thereby arriving at the minimum square error H for the symbol block and accumulating it in the ensemble average shown in (4) in order to obtain the estimated MER.

(g) Updating the instrument's reference constellation gain scale and its center frequency based on the most recent update of the estimates of $\hat{a}$ and $\hat{\Omega}$ respectively. This can be done by driving the gain scale in a direction and magnitude that makes $\hat{a}=1$ and the receiver tuning frequency such that $\hat{\Omega}=0$. These receiver parameters may be smoothed using running average techniques prior to their actual instrument update.

(h) Repeating all of the above steps for the next block of *N* consecutive symbols.

It can be shown (in an analysis that is beyond the scope of this paper) that although some of the steps described above are derived based on the assumption of zero additive noise, their programmatic results under noise conditions produce asymptotically stable and unbiased estimates. It can be further shown that both phase noise and the additive noise are fully and correctly accounted for in the resultant MER estimates.

In order to evaluate the effects of phase noise alone on the average MER measure, we shall proceed to evaluate the random variable *H* in (10) assuming zero additive noise (w_k=0). We shall average (4) over the ensemble of possible random transmission symbols Z_k and the ensemble of random phase deviations φ_k that are statistically independent of the transmission symbols Z_k. Hence, for zero additive noise in (2) we substitute V_k in (10) and obtain after combining and collecting terms:

$$\begin{aligned} H &= \sum_{k=1}^{N}|V_k|^2 - \left[\sum_{k=1}^{N}\operatorname{Re}\,(e^{i\hat{\varphi}_k} Z_k V_k^*)\right]^2 \Big/ \sum_{k=1}^{N}|Z_k|^2 = \sum_{k=1}^{N}|Z_k|^2 - \left[\sum_{k=1}^{N}|Z_k|^2\cos(\hat{\varphi}_k - \varphi_k)\right]^2 \Big/ \sum_{k=1}^{N}|Z_k|^2 \\ &= \sum_{k=1}^{N}\sum_{m=1}^{N}|Z_k|^2\,|Z_m|^2\,[1-\cos(\hat{\varphi}_k - \varphi_k)\cos(\hat{\varphi}_m - \varphi_m)] \Big/ \sum_{k=1}^{N}|Z_k|^2 \end{aligned} \tag{18}$$

As before, we assume that the actual phase deviations φ_k from the phase estimates $\hat{\varphi}_k$ are sufficiently small, permitting the expansion of the trigonometric expression in (18) and keeping only terms up to second order in $(\hat{\varphi}_k - \varphi_k)$ and in $(\hat{\varphi}_m - \varphi_m)$ while neglecting higher order terms. Upon performing one of the sums and collecting terms, we obtain the following

$$H \cong \sum_{k=1}^{N}(\hat{\varphi}_k - \varphi_k)^2|Z_k|^2 \tag{19}$$

Thus, we have proved that the least-squared-error estimate produces an expected result: The error energy is expressed as the accumulation of the magnitude-squared tangential deviations from the estimated constellation points when the angular deviations $(\hat{\varphi}_k - \varphi_k)$ are small. Using (4), we now obtain the MER due to phase noise alone as follows:

$$MER^{-1} \cong E\left[\sum_{k=1}^{N} (\hat{\varphi}_k - \varphi_k)^2 \left|Z_k\right|^2\right] \Big/ E\left[\sum_{k=1}^{N} \left|Z_k\right|^2\right] \tag{20}$$

It should be emphasized that we derived (20) using only the assumption of small phase deviations from an estimated phase trajectory $\hat{\varphi}_k$ without any assumption on how this trajectory is estimated. This result therefore applies *regardless of the method for obtaining the phase estimate trajectory* $\hat{\varphi}_k$. For MER measuring systems employing a demodulator with a continuous carrier phase tracking loop, the quantities $(\hat{\varphi}_k - \varphi_k)$ in (20) may be thought of as the untracked phase errors, the power of which is weighted by $|Z_k|^2$ in order to obtain the MER. It can be shown that if $(\hat{\varphi}_k - \varphi_k)^2$ and $|Z_k|^2$ were statistically uncorrelated and $(\hat{\varphi}_k - \varphi_k)$ a stationary process, (20) could be evaluated directly in a simple frequency domain analysis of the untracked phase error. This would be based on the product of the phase noise power spectrum density and the demodulator tracking loop transfer characteristics, integrated over frequency. This frequency domain approach had been adopted by others [5],[6],[7], implicitly invoking a statistical independence of $(\hat{\varphi}_k - \varphi_k)^2$ from $|Z_k|^2$. However, this implicit assumption lacks theoretical support, particularly since any phase estimates $\hat{\varphi}_k$ must necessarily be derived from the values of detected symbols Z_k and are, by definition, statistically dependent on them. In our case, that dependence is evident from (16). In contrast, our analysis below, takes into account any statistical correlations that exist between $(\hat{\varphi}_k - \varphi_k)^2$ and Z_k by inserting the estimation relations explicitly, thereby eliminating $\hat{\varphi}_k$ from the MER expression.

B. The effective phase-noise rejection filtering associated with a given measurement block size

In order to evaluate (20) and express the result in terms of the phase noise statistics alone, we must eliminate $\hat{\varphi}_k$ by using its value from (5) and (16):

$$\hat{\varphi}_k = \hat{\varphi}_0 + k\,\hat{\Omega} T_S = \frac{(\mu_2 - \mu_1 k)\sum_{m=1}^{N} \varphi_m \left|Z_m\right|^2 + (\mu_0 k - \mu_1)\sum_{m=1}^{N} m\,\varphi_m \left|Z_m\right|^2}{\mu_0\,\mu_2 - \mu_1^2} \tag{21}$$

Substituting the result of (21) in (19) we obtain:

$$H = \frac{\sum_{k=1}^{N}\sum_{m=1}^{N}(2\mu_1 k - \mu_0\, k\, m - \mu_2)\,\varphi_k\varphi_m\,|Z_k|^2\,|Z_m|^2}{\mu_0\,\mu_2 - \mu_1^2} + \sum_{k=1}^{N}\varphi_k^2\,|Z_k|^2 \tag{22}$$

This expression is further developed in Appendix II, wherein it is shown and concluded in (50) that for stationary phase noise and for $N >> 1$, its statistical expectation can be approximated using an integral of the continuous autocorrelation function of the phase noise $R_\varphi(\tau) = E[\varphi(t+\tau)\varphi(t)]$, with the following result:

$$MER^{-1} = \frac{E[H]}{N\langle Z^2\rangle} \cong R_\varphi(0) - \frac{4}{T^4}\int_0^T R_\varphi(\tau)(T-\tau)[T(T-\tau)-\tau^2]\,d\tau \tag{23}$$

wherein T is the total duration spanned by the N consecutive symbols in the measurement record.

Equation (23) is our central result and it shows that the inverse MER is equal to the total variance $R_\varphi(0)$ of the (zero mean) phase noise, minus a term related to the *removal* of phase drifts that are otherwise accounted for as an equivalent frequency offset during the epoch T. Thus, the kernel function given by $G(\tau) = (T-\tau)[T(T-\tau)-\tau^2]$ multiplying the phase noise autocorrelation function in the integrand of (23) contains an effective phase noise *filtering action* associated with the MER measurement instrument's phase trajectory estimation over a record duration of T seconds. A more useful and intuitive approach is to express (23) in the frequency domain. We note that the autocorrelation function of the phase noise can be obtained from the two sided phase noise spectral density $S_\varphi(\omega)$ by the inverse Fourier transform:

$$R_\varphi(\tau) = \int_{-\infty}^{+\infty} S_\varphi(\omega)\, e^{i\omega\tau}\, d\omega/(2\pi) \tag{24}$$

To see the filtering effect in an equivalent frequency domain view, we recall that the MER derivation from (48) in Appendix II relied on the even symmetry of the autocorrelation function stated in (46). This enables the even symmetry extension of $G(\tau)$ about $\tau = 0$ and thus (23) can be written over the interval $[-T, T]$ and subsequently transformed to the frequency domain using (24) as follows:

$$MER^{-1} = R_\varphi(0) - \frac{2}{T^4}\int_{-T}^{T} R_\varphi(\tau)G(|\tau|)d\tau = R_\varphi(0) - \frac{2}{T^4}\int_{-T}^{T}\left(\int_{-\infty}^{+\infty} S_\varphi(\omega)\, e^{i\omega\tau}\frac{d\omega}{2\pi}\right)G(|\tau|)d\tau$$
$$= \int_{-\infty}^{+\infty} S_\varphi(\omega)\frac{d\omega}{2\pi} - \int_{-\infty}^{+\infty} S_\varphi(\omega)\left(\frac{2}{T^4}\int_{-T}^{T} G(|\tau|)\, e^{i\omega\tau} d\tau\right)\frac{d\omega}{2\pi} = \int_{-\infty}^{+\infty} S_\varphi(\omega)F(\omega)\frac{d\omega}{2\pi} \tag{25}$$

where we have used Fubini's Theorem for changing the order of integration. As introduced above, the function $F(\omega)$ is defined based on $G(\tau)$ as follows:

$$F(\omega) = 1 - \frac{2}{T^4}\int_{-T}^{T} G(|\tau|)\, e^{i\omega\tau} d\tau = 1 - \frac{2}{T^4}\int_{-T}^{T} G(|\tau|)[\cos(\omega\tau) + i\sin(\omega\tau)]d\tau$$
$$= 1 - \frac{4}{T^4}\int_{0}^{T} G(\tau)\cos(\omega\tau)d\tau = 1 - \frac{4}{T^4}\int_{0}^{T}(T-\tau)[T(T-\tau)-\tau^2]\cos(\omega\tau)d\tau = \tag{26}$$
$$= 1 - \frac{4}{(\omega T)^2}\left[2 + \cos(\omega T) + 3\frac{\sin^2(\omega T/2)}{(\omega T/2)^2} - 6\frac{\sin(\omega T)}{\omega T}\right]$$

The function $F(\omega)$ can be viewed as the magnitude-squared frequency response of an *effective* carrier-tracking filter. The following observations from (26) are consistent with this view:

(a) As a squared magnitude function in the right hand side of (25), $F(\omega)$ is indeed positive for all frequencies and is an even function of frequency.

(b) By expanding the right hand side of (26) in a Taylor series about $\omega = 0$, it can be seen that as ω approaches zero, so does $F(\omega)$ and that it behaves asymptotically as a low frequency attenuator in accordance with:

$$F(\omega) = \frac{(\omega T)^4}{720} - \frac{(\omega T)^6}{25200} + \cdots \tag{27}$$

(c) Based on the first term in the above expansion, the effective filtering effect has an asymptotic corner frequency f_C meeting the condition $(2\pi f_C T)^4 / 720 = 1$, which corresponds to $f_C = 0.8244/T$.

(d) The frequency response in accordance with (26) is shown in Figure 1.

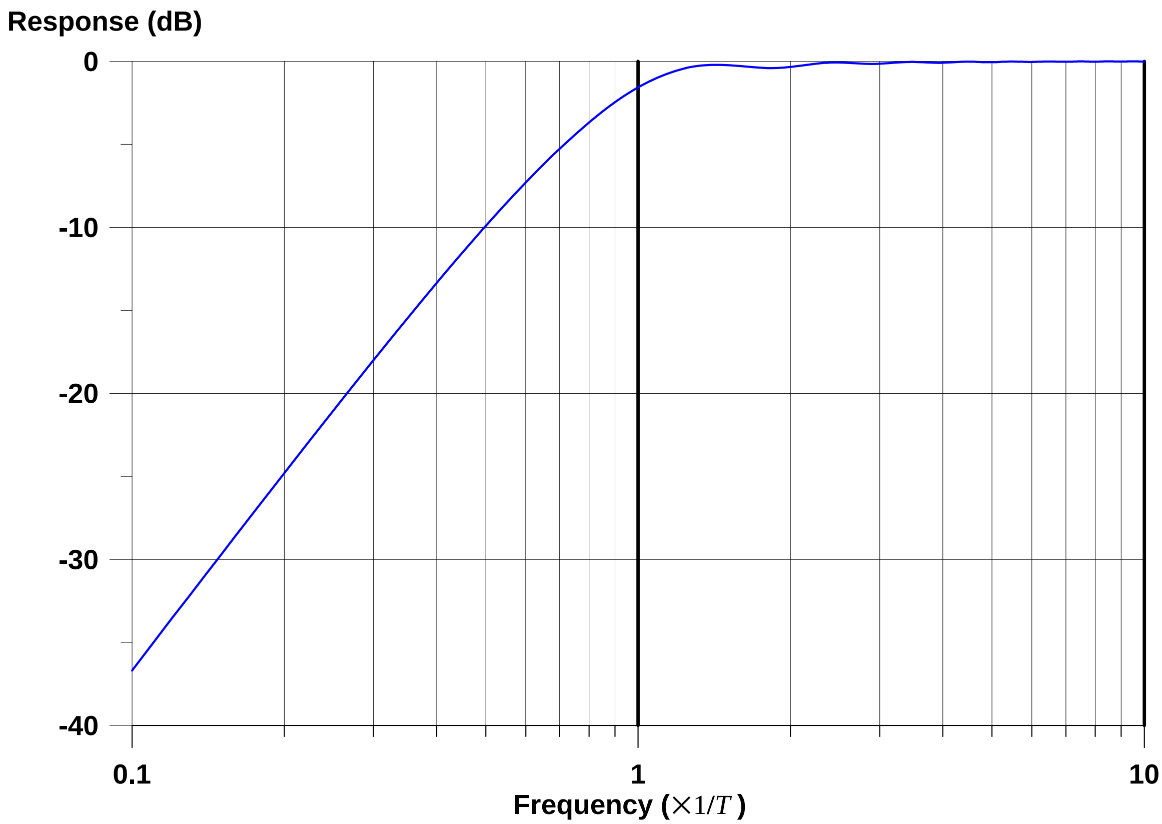

Figure 1. Magnitude squared frequency response $F(\omega)$ of the effective phase noise rejection filter due to least squared error MER estimates over a block of QAM symbols of duration T.

At low frequencies, the phase noise rejection performance of $F(\omega)$ is equivalent to that of a second-order carrier-tracking loop. Indeed, test results reporting this property in a commercial block based vector signal analyzer measurement set are reported in [8].

C. Application to a typical phase noise profile

The contribution to MER values due to degradations induced by phase noise as derived in (25) and (26) requires the specification of the phase noise spectral density $S_\varphi(\omega)$. For practical purposes, an analytical estimate for the phase noise contribution to MER can be derived for carrier oscillator phase noise spectral profiles having a square law decline with offset frequency over the frequencies of interest. The Lorentzian spectral density has such characteristic and it is the phase noise density of a free-running oscillator perturbed by white noise sources [9] [10]. Indeed, such spectral densities are typically observed over the offset frequency range that exceeds the phase locked loop bandwidth of synthesized oscillator sources (the free-running phase noise range).

The Lorentzian phase noise density is given by

$$S_\varphi(\omega) = R_\varphi(0)\frac{2\beta}{\omega^2+\beta^2} \tag{28}$$

where β is the Lorentzian angular corner frequency. Inserting the Lorentzian density from (28) and the function $F(\omega)$ from (26) into (25), we obtain[1]

$$\begin{aligned}
MER^{-1} &= 2\int_0^{+\infty} S_\varphi(\omega)F(\omega)\frac{d\omega}{2\pi} = \\
&= \int_0^{+\infty}\frac{4R_\varphi(0)\beta}{(\omega^2+\beta^2)}\left\{1-\frac{4}{(\omega T)^2}\left[2+\cos(\omega T)+3\frac{\sin^2(\omega T/2)}{(\omega T/2)^2}-6\frac{\sin(\omega T)}{\omega T}\right]\right\}\frac{d\omega}{2\pi} = \\
&= R_\varphi(0)\left\{(\beta T)^2\left[(\beta T)^2-4\beta T+8\right]+4\left[(\beta T)^2+6\beta T+6\right]\exp(-\beta T)-24\right\}\Big/(\beta T)^4 \\
&= R_\varphi(0)\left\{\frac{2\beta T}{15}-\frac{(\beta T)^3}{210}+\frac{(\beta T)^4}{720}+\cdots+\right\}
\end{aligned} \tag{29}$$

For applications in which the symbol rate $1/T_S$ is several MS/s, any practical MER analysis block length N would still make $T = N\,T_S$ sufficiently small compared to the effective Lorentzian relaxation time $1/\beta$. This means that $\beta T \ll 1$, and that we can neglect the high-order terms in (29), arriving at the approximation for phase noise contribution to MER up to second order in βT:

$$MER^{-1} \cong \frac{2}{15}R_\varphi(0)\beta T, \quad \text{for } \beta T \ll 1 \tag{30}$$

The equation above shows that under the foregoing assumptions, *the phase noise contribution to measured MER is only a small fraction of the total phase noise power* $R_\varphi(0)$ *and is inversely proportional to the duration of the measurement interval T over which the signal phase trajectory estimate is made.*

---

[1] The result in (29) can also be obtained directly by inserting the autocorrelation function of the Lorentzian density $R_\varphi(\tau) = R_\varphi(0)\exp(-\beta\,|\,\tau\,|)$ in (23) and performing the integration directly.

IV. IMPLICATIONS FOR MER SPECIFICATIONS AND TESTING

Whereas contributions to MER from modulation errors associated with distortion and additive noise are nominally independent of the measurement block duration, this does not hold for phase noise error contributions, which we have shown to increase with block duration. The first important conclusion from this analysis is that no repeatable and consistent MER measurement results can be prescribed or expected by merely stating MER requirements in a single dB specification. Such single number specification is essentially meaningless without a *second* accompanying parameter defining the measurement symbol block duration T or alternatively, the specific effective frequency response of the MER measurement set's demodulator carrier tracking system. Unfortunately, numerous specification documents for communications equipment that specify MER or EVM, do so without specifying this second essential parameter.

Figure 2 shows laboratory test results indicating that the second parameter is indeed essential. It shows test results for QAM signals having various levels of carrier phase noise and the corresponding measured MER values as a function of the number of symbols in a measurement block. Note the general plot region to the right wherein phase noise effects appear to dominate the MER results only for block lengths greater than several hundred symbols. Thermal noise, quantization noise and distortion make a baseline contribution to the resultant MER, thereby masking some of the initial phase-noise-induced decline in MER with increased block length.

The declines in MER values with reduction of block length N on the left side of the plots are inherent to the increased symbol fluctuation induced errors that are outside the scope of our model. These errors are in the decision-directed symbol sampling times and detected reference constellation points $\{Z_k\}_{k=1}^{N}$. In this regard, with short symbol records that fill only a fraction of all possible points in the constellation, there is a greater frequency of events having phase, amplitude and symbol-timing ambiguity, which erratically establish erroneous reference constellation points.

Figure 2 also shows the phase-noise-dominated MER decline for block lengths greater than 500 symbols for the consumer grade LO plot. It appears steeper than the –10 dB per decade predicted by our model in (30). This is similarly likely due to increased errors of the estimated constellation parameters (particularly symbol-timing errors) induced by increasing phase noise.

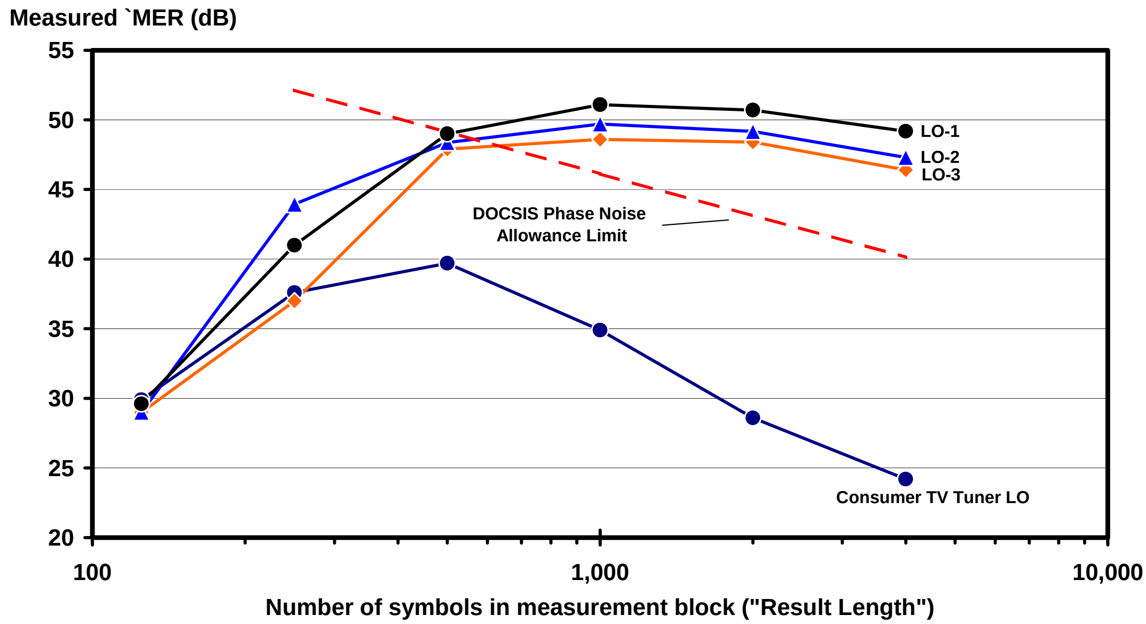

Figure 2. MER measurement results by symbol block size with various carrier local oscillators (LO). Results for three distinct CATV head-end grade LOs are designated with LO-1,2,3 as distinguished from that of a consumer grade TV tuner LO. Measurements were made with an Agilent PSA 4440A Vector Signal Analyzer for 256-QAM DOCSIS compliant signals with 5.36 MS/s. at a center frequency of 500 MHz.

A. *Matching MER measurement conditions to end-user demodulator characteristics*

In order that MER measurements of downstream sources provide effective characterization of transmitter impairments including its phase noise, it is preferable to set the measurement block length T of the MER measurement system so that it matches actual carrier tracking loops' characteristics of reference end-user demodulators. This practice is important for characterizing the actual MER or SNR margin that a particular transmitter's phase noise provides for a specified end-user demodulator. For consumer digital cable demodulators operating at 64 QAM, the reported carrier tracking loop response is of second order with a corner frequency of f_C = 8 kHz [5]. According to the results herein, the equivalent block period is therefore given by $T = 0.8244 / f_C$ and the corresponding number of symbols for a 64 QAM symbol rate of 5.057 MS/s is given by $N = 0.8244\, f_S / f_C = 521$ symbols. It is not surprising that this resulting block length (and the corresponding corner frequency) is also optimal for the phase noise characteristics of a consumer tuner as seen in Figure 2. This is likely because carrier tracking loop bandwidths reported for consumer demodulators in [5] were likely optimized for the particular phase noise performance of their consumer grade tuners and those demodulator carrier tracking loop bandwidths are set for minimum effective demodulated constellation errors. Fortunately, the LO-1 through LO-3 plots in Figure 2 shows that these head-end sources' phase noise contributions in of themselves practically do not impair the MER margin for such tracking loop corner frequencies.

B. Application to MER specifications in DOCSIS

DOCSIS sets forth the requirements of the cable industry for QAM transmission equipment used on cable systems in the U.S. and Europe. In 2005, the DOCSIS working group that developed its Downstream RF Interface Specification (DRFI) [11] sought to replace several in-band modulation distortion specifications with a single MER specification for greater efficiency in compliance testing. This author's written contributions to the DRFI Working Group was an earlier version of this paper and an analysis of the various degradation components that contribute to MER [12]. Both showed that MER specifications must be consistent with the DOCSIS phase noise allowance specifications. The DOCSIS legacy RF Interface specifications permits downstream QAM transmitter phase noise up to the levels listed in Table 1.

Frequency Offset Band		Double Sided Integrated Noise Power
Band 1	1 kHz - 10 kHz:	-33 dBc
Band 2	10 kHz - 50 kHz:	-51 dBc
Band 3	50 kHz - 3 MHz:	-51 dBc

Table 1 Downstream phase noise DOCSIS specifications. *Source*: Table 6-3, DRFI [11].

By its very nature, the lack of a specific *functional* dependence on offset frequency precludes this type of integrated phase noise specification from uniquely predicting the effect on measured MER for a device operating at the compliance limit. However, based on practical considerations and certain approximations, reliable estimates for MER limits implied by the DOCSIS phase noise allowance can be obtained. To obtain these limits, we note that over the offset frequency range of interest, the source phase noise density can be approximated by a square-law decline, as obtained for $\omega \gg \beta$ in (28):

$$S_\varphi(\omega) \cong 2R_\varphi(0)\beta\,\omega^{-2} \tag{31}$$

Therefore, the maximum allowable value of $R_\varphi(0)\beta$ is a constant that can be determined by integrating (31) over the frequency band of interest and equating the result to a specified (or measured) integrated phase noise value in that band. With this spectral density, the double-sided integrated phase noise power between offset band edge frequencies f_L and f_H is given by:

$$\sigma_\varphi^2(f_L, f_H) = 2\int_{2\pi f_L}^{2\pi f_H} S_\varphi(\omega)d\omega/2\pi \cong \frac{R_\varphi(0)\beta}{\pi^2}\int_{f_L}^{f_H} f^{-2}df = \frac{R_\varphi(0)\beta}{\pi^2}\left(\frac{f_H - f_L}{f_H f_L}\right) \tag{32}$$

We now note that whereas the specification in Table 1 restricts phase noise power in Band 2 to a level 18 dB below that allowed in Band 1, the integration factor $(f_H - f_L)/f_H f_L$ in (32) for Band 2 amounts to only 10.5 dB in relative reduction of integrated phase noise power. This implies that the maximum allowable value of $R_\varphi(0)\beta$ is determined by the limit in Band 2. This conclusion can be verified by similarly examining the relatively more relaxed specification (for this Lorentzian density) in Band 3. Using f_L = 10 kHz, f_H = 50 kHz and the –51 dBc limit for $\sigma_\varphi^2(f_L, f_H)$ in Band 2, (32) yields the maximum allowed value $R_\varphi(0)\beta = 0.98\,\text{s}^{-1}$. This result[2] sets the upper limit on observed MER of devices operating at the DOCSIS phase noise compliance limit (shown for f_S = 5.3 MS/s in the broken line of Figure 2):

$$\text{DOCSIS Phase Noise Limited MER } = $$
$$= 10\log(MER_D) \approx -10\log_{10}\left[\frac{2}{15}R_\varphi(0)\beta T\right] = -10\log_{10}\left[0.131\text{s}^{-1}\times N/f_S\right]$$

Hence, the DOCSIS specification of 43 dB for equalized MER (Table 6-3, DRFI [11]) provides necessary margin for additional impairments other than phase noise. The exclusion in the DRFI MER specifications of noise within 50 kHz of the carrier frequency cannot be fully utilized by practical MER measurement sets because raising the measurement corner frequency to such frequency requires setting N to unusable short block lengths of approximately 85 symbols.

[2] This numerical result is half of that used erroneously in [12] due to its error in the counterpart equation of (31).

Nevertheless, this specification affirmatively provides full flexibility in selecting practical symbol block lengths for compliance verification and testing.

C. Implications for MER Measurement Instruments' Specifications

MER measurement instruments employ internal receivers and associated synthesized LO sources. These sources' own phase noise contributes to the observed MER results, setting a ceiling on possible MER measurement results and therefore must be taken into account. Unfortunately, as of this writing, this author is aware of no commercial MER measurement set having adequate specifications that specifies its MER or EVM measurement performance limits *as a function of* symbol block length or carrier tracking loop bandwidth settings. Often, a single (conservatively specified) MER value is guaranteed, perhaps applicable for a full range of measurement block periods. However, the usability of these vendors' specifications is dubious at best, having values that are often lower than the specifications required in modern high order constellations such as DOCSIS. This deficiency frustrates the proper design, planning and automation of MER compliance testing.

It is hoped that this paper would encourage vendors to correct these deficiencies in their MER measurement products' specifications. In order to avoid specifying internal sources' phase noise profiles, vendors should provide a specification of an *MER mask* that identifies an MER limit as a function of symbol block length or carrier tracking loop bandwidth settings. A mask of this type can appropriately reflect the internal phase noise profile limits, thereby facilitating useful overall MER measurement capability of such instruments.

APPENDIX I. CERTAIN STATISTICAL MOMENTS OF QAM CONSTELLATIONS

Here we evaluate certain even statistical moments of the transmitted symbols Z_k given in (1):

$$Z_k = p_k d + i q_k d \quad p_k = \pm 1, \pm 3, \pm 5, \pm 7, ...; \; q_k = \pm 1, \pm 3, \pm 5, \pm 7, ...; \text{ and where } i = \sqrt{-1} \tag{1}$$

We assume that the random integers p_k and q_k are uncorrelated and that each outcome in their respective range is equally likely. The average power in the constellation is its second moment, which we denote by $\langle Z^2 \rangle$. Due to the four-quadrant symmetry, it can be found by averaging the square magnitude of all possible n^2 symbols within one quadrant of the QAM constellation:

$$\langle Z^2\rangle \equiv E\left\{\left|Z_k\right|^2\right\} = \frac{1}{n^2}\sum_{j=1}^{n}\sum_{m=1}^{n}\left[(2j-1)^2 d^2 + (2m-1)^2 d^2\right] = \frac{2d^2(4n^2-1)}{3} \tag{33}$$

Similarly, the forth moment, which we denote by $\langle Z^4\rangle$, can be found by averaging the forth power of the magnitudes of all possible n^2 symbols of one quadrant of the QAM constellation:

$$\langle Z^4\rangle \equiv E\left\{\left|Z_k\right|^4\right\} = \frac{1}{n^2}\sum_{j=1}^{n}\sum_{m=1}^{n}\left[(2j-1)^2 d^2 + (2m-1)^2 d^2\right]^2 = \frac{4d^4(4n^2-1)(28n^2-13)}{45} \tag{34}$$

It is often useful to express the higher moment $\langle Z^4\rangle$ in terms of the constellation average power, the second moment $\langle Z^2\rangle$. It turns out that by using (33) and (34), one can show that the relationship between $\langle Z^4\rangle$ and $\langle Z^2\rangle$ is approximately independent of the QAM constellation size and that the following asymptotic relation holds as the symbol decision region power d^2 is small compared to the full constellation power:

$$\langle Z^4\rangle = \frac{2d^2\langle Z^2\rangle\left(28n^2-13\right)}{15} = \frac{\langle Z^2\rangle\left(7\langle Z^2\rangle - 4d^2\right)}{5} \cong \frac{7}{5}\langle Z^2\rangle^2 \text{ when } d^2 << \langle Z^2\rangle \tag{35}$$

We use the right hand side approximation above for large order constellations such as 64 QAM, 256 QAM, and 1024 QAM.

A. Joint moments

For bivariate joint moments, the fact that Z_k is uncorrelated with Z_m whenever $k \neq m$, leads to the following simple expression based on the constellation's fourth-order moment result in (35):

$$\langle |Z_k|^2 |Z_m|^2\rangle = E\left[|Z_k|^2 |Z_m|^2\right] = \langle Z^2\rangle^2\left(1+\frac{2}{5}\delta_{k,m}\right) \text{ ; where } \delta_{k,m} \text{ is the Kronecker Delta} \tag{36}$$

We now turn to the trivariate joint moments of the form $\langle |Z_r|^2 |Z_k|^2 |Z_m|^2\rangle = E\left\{|Z_r|^2 |Z_k|^2 |Z_m|^2\right\}$ for possibly distinct symbol indices *r*, *k*, and *m*, and derive these moments in terms of the univariate moments $\langle Z^{2j}\rangle \equiv E\left\{|Z_k|^{2j}\right\}$, $j = 1, 2, 3$. To do so, we make use of conditional expectation identities and the newly defined random variables Y_m and $U_{k,m}$ as follows:

$$
\begin{aligned}
&E\left[X_r X_k X_m\right]=E\left\{E\left[X_r X_k \left|X_m\right.\right]X_m\right\}=E\left[Y_m X_m\right], \text{ where}\\
&Y_m=E\left[X_r X_k \left|X_m\right.\right]=E\left\{E\left[X_r \left|X_k ; X_m\right.\right]X_k \left|X_m\right.\right\}=E\left[U_{k,m} X_k \left|X_m\right.\right], \text{ where}\\
&U_{k,m}=E\left[X_r \left|X_k ; X_m\right.\right]
\end{aligned}
\tag{37}
$$

For jointly uncorrelated random variables X_j, we directly obtain the following property for $U_{k,m}$:

$$
U_{k,m}=E\left[X_r \left|X_k ; X_m\right.\right]=\begin{cases} E\left[X_r\right] \text{ , whenever } r \neq k \text{ and } r \neq m \\ X_k \text{ , whenever } r=k \\ X_m \text{ , whenever } r=m \text{ and } r \neq k \end{cases}
\tag{38}
$$

Identifying $X_j \equiv \left|Z_j\right|^2$ for $j = r, k, m$ in our case, we write (38) as follows:

$$
U_{k,m}=E\left[\left|Z_r\right|^2 \mid Z_k ; Z_m\right]=\langle Z^2\rangle+\delta_{r,k}\left(\left|Z_k\right|^2-\langle Z^2\rangle\right)+\delta_{r,m}\left(1-\delta_{r,k}\right)\left(\left|Z_m\right|^2-\langle Z^2\rangle\right)
\tag{39}
$$

Substituting this expression for $U_{k,m}$ in (37), using conditional expectation identities as in (38), and collecting terms, we obtain

$$
\begin{aligned}
E\left\{\left|Z_r\right|^2\left|Z_k\right|^2\left|Z_m\right|^2\right\}&=\langle Z^6\rangle\delta_{r,k,m}+\langle Z^2\rangle\langle Z^4\rangle\left[\delta_{r,k}\left(1-\delta_{k,m}\right)+\delta_{r,m}\left(1-\delta_{k,m}\right)+\delta_{k,m}\left(1-\delta_{r,k}\right)\right]\\
&\quad+\langle Z^2\rangle^3\left[1-\delta_{r,k}-\delta_{r,m}\left(1-\delta_{k,m}\right)-\delta_{k,m}\left(1-\delta_{r,k}\right)\right]\\
&=\delta_{r,k,m}u_3+\left(\delta_{r,k}+\delta_{r,m}+\delta_{k,m}\right)u_2+u_1, \text{ whith the following definitions:}
\end{aligned}
\tag{40}
$$

$$
\begin{aligned}
&u_1=\langle Z^2\rangle^3; u_2=\langle Z^2\rangle\left(\langle Z^4\rangle-\langle Z^2\rangle^2\right); u_3=\langle Z^6\rangle+\langle Z^2\rangle\left(2\langle Z^2\rangle^2-3\langle Z^4\rangle\right) \text{ and wherein}\\
&\delta_{r,k,m}=\delta_{r,k}\delta_{r,m}=\delta_{k,m}\delta_{r,k}=\delta_{k,m}\delta_{r,m}
\end{aligned}
$$

For use in the text, the expression for u_2 can be simplified based on the specific asymptotic value of the fourth moment in (35): $u_2=\langle Z^2\rangle\left(\langle Z^4\rangle-\langle Z^2\rangle^2\right)\cong\langle Z^2\rangle\left((7/5)\langle Z^2\rangle^2-\langle Z^2\rangle^2\right)=2\langle Z^2\rangle^3/5$

APPENDIX II. DERIVATION OF PHASE ERROR POWER

We derive here the phase noise power of what MER instruments ascribe to phase fluctuations about their estimated linear phase trajectory of a transmitted QAM signal. For a given measurement record of N consecutive symbols, the sample phase error power H is derived in the text in (22), wherein all the terms used in the equation below have their defined meaning as in the text.

$$H = \frac{\sum_{k=1}^{N}\sum_{m=1}^{N}(2\mu_1 k - \mu_0\, k\, m - \mu_2)\,\varphi_k\varphi_m \left|Z_k\right|^2 \left|Z_m\right|^2}{\mu_0\ \mu_2 - \mu_1^2} + \sum_{k=1}^{N}\varphi_k^2 \left|Z_k\right|^2 \tag{22}$$

The random variable in the denominator of (22) has a mean value given by:

$$E\left[\mu_0\ \mu_2 - \mu_1^2\right] = \sum_{k=1}^{N}\sum_{m=1}^{N} k(k-m)E\left[\left|\,Z_k\right|^2 \left|\,Z_m\right|^2\right] = \langle\, Z^2 \rangle^2\ \frac{N^2(N^2-1)}{12} \tag{41}$$

It can be shown that for sufficiently large N, the variance-to-mean-squared ratio of this denominator approaches zero as $1/N$. Thus, for large values of N, the expectation of the quotient in (22) can be replaced by the quotient of the expectations as follows:

$$E\left[H\right] = \frac{\sum_{k=1}^{N}\sum_{m=1}^{N}\langle\left(2\mu_1 k - \mu_0\, k\, m - \mu_2\right)\left|Z_k\right|^2\left|Z_m\right|^2\rangle\langle\varphi_k\varphi_m\rangle}{\langle\, Z^2\rangle^2\ [N^2(N^2-1)/12]} + \sum_{k=1}^{N}\langle\varphi_k^2\rangle\langle\left|Z_k\right|^2\rangle\ ; \tag{42}$$

where the brackets $\langle\bullet\rangle$ denote the statistical expectation and where the statistical independence of the random complex symbols and the random phases is assumed. We now note that the term $\langle\varphi_k\varphi_m\rangle$ used in (42) is the autocorrelation function of the phase noise, assuming the measurement demodulator is phase locked to the transmitted signal. It is denoted by

$$\langle\varphi_k\varphi_m\rangle = E\left[\varphi_k\varphi_m\right] = R_\varphi(k,m) \tag{43}$$

Recognizing that the record moments μ_j are random variables constructed from the complex symbols Z_k in accordance with (15), we observe that the double sum numerator in (42) is in fact a function of the trivariate moments of Z_k and is therefore given by

$$\sum_{k=1}^{N}\sum_{m=1}^{N}\langle\left(2\mu_1 k-\mu_0\, k\, m-\mu_2\right)|Z_k|^2|Z_m|^2\rangle\langle\varphi_k\varphi_m\rangle=\sum_{k=1}^{N}\sum_{m=1}^{N}\sum_{r=1}^{N}\left(2rk-km-r^2\right)\langle|Z_r|^2|Z_k|^2|Z_m|^2\rangle\langle\varphi_k\varphi_m\rangle$$
$$=\sum_{k=1}^{N}\sum_{m=1}^{N}\sum_{r=1}^{N}\left(2rk-k\,m-r^2\right)\left[\delta_{r,k,m}u_3+\left(\delta_{r,k}+\delta_{r,m}+\delta_{k,m}\right)u_2+u_1\right]R_\varphi(k,m)$$
$$=u_3\sum_{k=1}^{N}\left(2k^2-k^2-k^2\right)R_\varphi(k,k)+$$
$$+u_2\left(\sum_{k=1}^{N}\sum_{m=1}^{N}\left[\left(2k^2-k\,m-k^2\right)+\left(2mk-k\,m-m^2\right)\right]R_\varphi(k,m)+\sum_{k=1}^{N}\left(2k\sum_{r=1}^{N}r-k^2N-\sum_{r=1}^{N}r^2\right)R_\varphi(k,k)\right)\quad(44)$$
$$+u_1\sum_{k=1}^{N}\sum_{m=1}^{N}\left(2k\sum_{r=1}^{N}r-N\,k\,m-\sum_{r=1}^{N}r^2\right)R_\varphi(k,m)$$
$$=u_2\left[\sum_{k=1}^{N}\sum_{m=1}^{N}\left(k^2-m^2\right)R_\varphi(k,m)+\sum_{k=1}^{N}[kN(N+1)-k^2N-N(N+1)(2N+1)/6]R_\varphi(k,k)\right]$$
$$+u_1\sum_{k=1}^{N}\sum_{m=1}^{N}\left(kN(N+1)-N\,k\,m-N(N+1)(2N+1)/6\right)R_\varphi(k,m)$$

To evaluate the triple sum above, we made use of (40), the expression for the trivariate moments in Appendix I, and the following summation identities:

$$\sum_{k=1}^{N}k^j=\begin{cases}N\ ;\ \text{for } j=0\\ N(N+1)/2\ ;\ \text{for } j=1\\ N(N+1)(2N+1)/6\ ;\ \text{for } j=2\end{cases}\qquad(45)$$

We now assume that the phase noise is stationary in the mean-square sense. This means that its autocorrelation function has the following property:

$$R_\varphi(k,m)=R_\varphi(m,k)=R_\varphi(|\,k-m\,|)\qquad(46)$$

Using this stationarity property and (44), we write (42) after substitution and canceling of terms as follows:

$$
\begin{aligned}
E[H] &= \Big\{ u_2 R_\varphi(0) \sum_{k=1}^{N} [kN(N+1) - k^2 N - N(N+1)(2N+1)/6] \\
&+ u_1 \sum_{k=1}^{N}\sum_{m=1}^{N} \big(kN(N+1) - N\,k\,m - N(N+1)(2N+1)/6\big) R_\varphi(k,m) \Big\} \Big/ \langle Z^2\rangle^2\, [N^2(N^2-1)/12] \\
&+ N\, R_\varphi(0)\langle Z^2\rangle = \Big\{ u_2 N R_\varphi(0) \big[N(N+1)(N+1)/2 - N(N+1)(2N+1)/3 \big] \\
&+ u_1 N \sum_{k=1}^{N}\sum_{m=1}^{N} \big(k(N+1-m) - (N+1)(2N+1)/6\big) R_\varphi(k,m) \Big\} \Big/ \langle Z^2\rangle^2\, [N^2(N^2-1)/12] + N\, R_\varphi(0)\langle Z^2\rangle \\
&= \frac{-u_2 N(N^2-1) R_\varphi(0)/6 + u_1 \sum_{k=1}^{N}\sum_{m=1}^{N} \big(k(N+1-m) - (N+1)(2N+1)/6\big) R_\varphi(k,m)}{\langle Z^2\rangle^2\, [N(N^2-1)/12]} + N\, R_\varphi(0)\langle Z^2\rangle \\
&= \frac{-\langle Z^2\rangle N(N^2-1) R_\varphi(0)/15 + \langle Z^2\rangle \sum_{k=1}^{N}\sum_{m=1}^{N} \big(k(N+1-m) - (N+1)(2N+1)/6\big) R_\varphi(k,m)}{[N(N^2-1)/12]} + N\, R_\varphi(0)\langle Z^2\rangle \\
&= \frac{12\langle Z^2\rangle \sum_{k=1}^{N}\sum_{m=1}^{N} \big[k(N+1-m) - (N+1)(2N+1)/6\big] R_\varphi(k,m)}{N(N^2-1)} + \left(N - \frac{4}{5}\right) R_\varphi(0)\langle Z^2\rangle
\end{aligned} \tag{47}
$$

wherein the values for u_1 and u_2 from Appendix I were substituted. The assumption of stationarity for the autocorrelation $R_\varphi(k,m) = R_\varphi(|k-m|)$ renders its value constant along the lines k - m = *const*. Exploiting this fact, the double sum in (47) can be converted into two single sums by changing variables and summing diagonally in the k - m index space parallel to the $m = k$ line. Using an index l defined by $m = k+l$ in a first sum and by $m = k - l$ in a second sum, the resulting summations are in the triangular regions above and below the line $m = k$ respectively:

$$
\begin{aligned}
E[H] = \frac{12\langle Z^2\rangle}{N(N^2-1)} &\left\{ \sum_{l=1}^{N-1}\sum_{k=l+1}^{N}\{k[N+1-(k-l)]-(N+1)(2N+1)/6\} R_\varphi(k,k-l) \right. \\
&\left. + \sum_{l=1}^{N-1}\sum_{k=1}^{N-l}\{k[N+1-(k+l)]-(N+1)(2N+1)/6\} R_\varphi(k,k+l) \right\} \\
&+\left(N-\frac{4}{5}\right)R_\varphi(0)\langle Z^2\rangle \\
= \frac{12\langle Z^2\rangle}{N(N^2-1)} \sum_{l=1}^{N-1} R_\varphi(l) &\left[\sum_{k=l+1}^{N}\{k[N+1-(k-l)]-(N+1)(2N+1)/6\} \right. \\
&\left. + \sum_{k=1}^{N-l}\{k[N+1-(k+l)]-(N+1)(2N+1)/6\} \right] \\
&+\left(N-\frac{4}{5}\right)R_\varphi(0)\langle Z^2\rangle \\
= \frac{12\langle Z^2\rangle}{N(N^2-1)} \sum_{l=1}^{N-1} R_\varphi(l) &\frac{(N-l)(l^2+Nl-N^2+1)}{3} + \left(N-\frac{4}{5}\right)R_\varphi(0)\langle Z^2\rangle
\end{aligned} \tag{48}
$$

As a good approximation in cases where *N* is large ($N >> 1$), we replace in (48) every occurrence of the terms N^2-1 by N^2 and replace $N-1$ or $N-4/5$ by *N* to arrive at

$$
E[H] = \langle Z^2\rangle \left[R_\varphi(0)N - \frac{4}{N^3}\sum_{l=1}^{N} R_\varphi(l)(N-l)[N(N-l)-l^2] \right] \tag{49}
$$

Because the symbol time granularity T_S is much smaller than the time period over which the phase noise autocorrelation function $R_\varphi(l)$ declines in value, we can express the sum over *l* in (49) as a time integral by way of the limit of a Riemann sum. To do so, we set the time increments $\Delta\tau = T_S$ so that $\tau = l\cdot\Delta\tau$ and so that $N\Delta\tau = NT_S = T$, wherein *T* is the total time over which a block of *N* consecutive symbols are received for analysis. The autocorrelation $R_\varphi(l)$ of phases that are *l* symbol-times apart, i.e. $\tau = l\cdot\Delta\tau$ seconds apart, is identified as equal to $R_\varphi(\tau)$. In this way, we rewrite the MER equation (20) using (49) divided by $N\langle Z^2\rangle$ and by passing to the integral limit as follows:

$$MER^{-1} = \frac{E[H]}{N\langle Z^2\rangle} = R_\varphi(0) - \frac{4}{N^4(\Delta\tau)^4}\sum_{l=1}^{N} R_\varphi(l)(N\Delta\tau - l\Delta\tau)[N\Delta\tau(N\Delta\tau - l\Delta\tau) - (l\Delta\tau)^2]\cdot\Delta\tau$$
$$\cong R_\varphi(0) - \frac{4}{T^4}\int_0^T R_\varphi(\tau)(T-\tau)[T(T-\tau)-\tau^2]d\tau \qquad (50)$$

ACKNOWLEDGEMENT

The author wishes to thank Mr. Cong Nguyen for making and compiling the MER measurements reported in this paper. These measurements were made at Broadband Innovations, Inc.

REFERENCES

[1] Agilent Technologies, "Using Error Vector Magnitude measurements to analyze and troubleshoot vector-modulated signals", Product Note PN 89400-14, Available at http://cp.literature.agilent.com/litweb/pdf/5965-2898E.pdf

[2] Apostolos Georgiadis, "Gain, phase imbalance, and phase noise effects on Error Vector Magnitude", *IEEE Transactions on Vehicular Technology*, Volume 53, No. 2, pp. 443 - 449 (March 2004).

[3] J.L. Pinto and I. Darwazeh, "Error Vector Magnitude relation to magnitude and phase distortion in 8-PSK systems", *Electronics Letters*, Vol. 27, No. 7, (March 29, 2001).

[4] Raymond A. Birgenheier and Richard P. Ryan, "Method and apparatus for measuring modulation accuracy", US Patent No. 5,187,719, (February 16, 1993).

[5] Mark Kolber, "Predict phase-noise effects in digital communication systems", *Microwaves & RF*, Vol. 38, No. 9, Sept. 1999, pp 59-70.

[6] Douglas Barker, "The effects of phase noise on high-order QAM systems", *Communications System Design Magazine*, (October, 1999). Available at http://www.commsdesign.com/main/1999/10/9910feat3.htm

[7] Gérard Terreault, "QAM signal impairments and their effects on MER and BER", Sunrise Telecom (2003). Available at http://www.sunrisetelecom.com/broadband/QAM_Impairment_Effects_on_MER_BER_104.pdf

[8] Matthew Sherman, "Comments on MER definition, test procedure, and requirements for QAM constellations using HP 89441A", Submission to IEEE 802.14a Hi-PHY (1999).

[9] D. B. Leeson, "A simple model of feedback oscillator noise spectrum", *Proc. IEEE*, vol. 54, No. 2, pp. 329-330, (February, 1966).

[10] Alper Demir, Amit Mehrotra, and Jaijeet Roychowdhury, “Phase noise in oscillators: A unifying theory and numerical methods for characterization”, *IEEE Transactions on Circuits and Systems I: Fundamental Theory and Applications*, vol. 47, no. 5, pp. 655 –674, (May 2000).

[11] CableLabs, “Data-Over-Cable Service Interface Specifications - Downstream RF Interface specification”, CM-SP-DRFI-I06-080215. Available at http://www.cablemodem.com/specifications/d-rfi.html.

[12] Ron D. Katznelson, “The technical requirements for multichannel QAM RF modulators”, *NCTA Technical Proceedings*, New Orleans, May 3, (2004).

Ron D. Katznelson received a dual BSc. degree in Mathematics and Physics in 1975 and the MSc. degree in Applied Semiconductor Physics in 1977, both from the Hebrew University in Jerusalem, Israel. He received his Ph.D. degree in Electrical Engineering (communication theory and systems) in 1982 from the University of California, San Diego, USA.

He is the Founder and President of Bi-Level Technologies in Encinitas, CA USA. From 1990 to 2005, he was Chief Technology Officer, Founder and Chairman of Broadband Innovations, (formerly known as MCSI). From 1983 to 1989, he was with the VideoCipher Division of M/A-COM Linkabit Corp., later acquired by General Instrument Corp., where he served as Director, New Technology Development. From 1982 to 1985, he was a Professor of Electrical Engineering at the University of California, San Diego. He authored numerous published articles and he is the coauthor of the book entitled “Electric Fields of the Brain” (New York, Oxford University Press, 1981). He is a named inventor in more than 25 U.S. patents and his research interests include optimal signal design, digital RF signal processing, digital television, signal representation & sampling theory, intellectual property management and patent law.

Dr. Katznelson was a member of CableLabs’ DOCSIS Working Group and a coauthor of its Downstream RF Interface Specifications. Dr. Katznelson is an advisor to high technology firms, a member of the University of California Library Advisory Board, and a member of the San Diego Intellectual Property Law Association.